

Nitridated Fibrous Silica (KCC-1) as a Sustainable Solid Base Nanocatalyst

Mohamed Bouhrara,[†] Chanakya Ranga,[†] Aziz Fihri,[†] Rafik R. Shaikh,[†] Pradip Sarawade,[†] Abdul-Hamid Emwas,[†] Mohamed N. Hedhili,[†] and Vivek Polshettiwar^{*,‡}

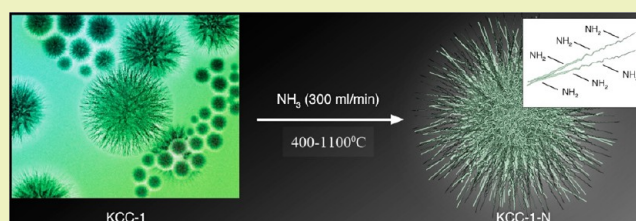
[†]Nanocatalysis Laboratory (NanoCat), King Abdullah University of Science and Technology (KAUST), Thuwal, Kingdom of Saudi Arabia

[‡]Nanocatalysis Laboratory (NanoCat), Tata Institute of Fundamental Research (TIFR), Mumbai, India

S Supporting Information

ABSTRACT: We observed that support morphology has dramatic effects on the performance of nitridated silica as a base. By simply replacing conventional silica supports (such as SBA-15 and MCM-41) with fibrous nanosilica (KCC-1), we observed multifold enhancement in the catalytic activity of the nitridated solid base for Knoevenagel condensations and transesterification reactions. This enhancement of the activity can be explained by amine accessibility, which is excellent in KCC-1 due to its open and flexible fibrous structure, that facilitates penetration and interaction with basic amine sites.

KEYWORDS: Nanocatalysis, Fibrous silica, KCC-1, Shape and morphology, Solid base, Knoevenagel condensation, Trans-esterification



INTRODUCTION

Solid bases have attracted considerable interest for potential applications as catalysts in important industrial processes, especially for petrochemical and fine chemical syntheses.^{1–7} Nitridation, the incorporation of nitrogen by treating a solid with ammonia gas at high temperatures, has been an effective approach for developing new solid base materials.^{8–11} The basicity of these nitrogen-containing materials was attributed to terminal NH₂ and bridging NH groups on the surfaces of these materials.^{12,13} This nitridation process was extended to mesoporous silica materials, such as MCM-41 and SBA-15, and a new class of nitrogen-substituted solid-base materials with high surface areas was developed.^{14–28} Although these new materials possess promising basicity, their activity is limited to a few substrates due to the restricted accessibility of amines, which are mainly present in the pores of these materials. In fact, these nitridated materials were not able to catalyze Knoevenagel condensation reactions between benzaldehyde and diethyl malonate, which is often used as a probing reaction to evaluate solid base catalysts.^{14–26} This inability to catalyze Knoevenagel reactions was due to the confined architecture of these solids where basic amine sites were located in pores, which restricted reactants from interacting with amines. Recently, Ougra et al. reported that they enhanced basicity by simply methylating nitridated SBA-15 and MCM-41.²⁹ According to Ougra et al., these materials catalyze Knoevenagel condensation reactions of challenging substrates. However, they used toxic methyl iodide and corrosive potassium carbonate to methylate amines. Therefore, there is a need for

a green sustainable solid base with better activity and accessibility.

We recently discovered a new silica (KCC-1) with a high surface area and excellent physical and textural properties.^{30–34} KCC-1 has novel fibrous morphologies, and its high surface area is due to these fibers and not pores.³⁰ Therefore, KCC-1 can be very useful as a catalyst support, in which there is a need for significant accessibility to active sites.^{31–34} In this paper, we report our results for ammoniated KCC-1 as a solid base with superior activity compared to other nitridated solid bases as well as recently developed N-methylated SBA-15 or MCM-41.²⁹ Surprisingly, the unique fibrous morphology of KCC-1 enabled the performance of this material without chemical modifications of nitridated materials.

EXPERIMENTAL SECTION

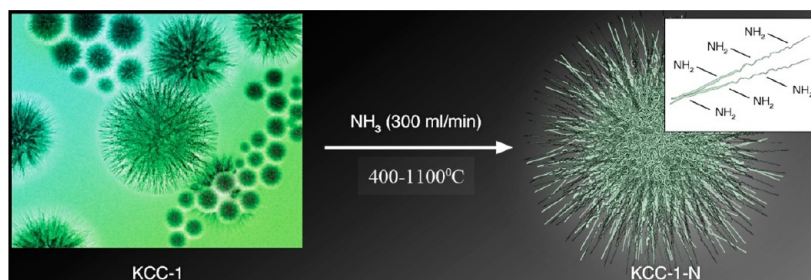
Nitridation of KCC-1. KCC-1 was synthesized using reported process with optimized reaction time of 30 min.³⁰ Nitridation was performed using a plug-flow fixed-bed quartz reactor. Typically, 1.5 g of KCC-1 was loaded in the quartz reactor. Then the reactor was purged with a 200 mL/min flow of argon, and the furnace was heated to 110 °C at a ramp rate of 5 °C/min in argon. The gas flow was changed to pure ammonia (300 mL/min) and maintained for 12 h at the desired temperature (from 400 to 1100 °C). The furnace was cooled to 150 °C. Then the gas flow was changed to 200 mL/min of argon, and the furnace was cooled to room temperature.

Received: April 29, 2013

Revised: June 22, 2013

Published: July 3, 2013

Scheme 1. Nitridation of KCC-1



Knoevenagel Condensation. Reactions were carried out in a Schlenk tube under argon. A mixture of 5 mmol of aldehyde, 6 mmol of active methylene substrates, and 30 mg of nanocatalyst (KCC-1-N500) in ethanol (10 mL) was stirred at room temperature for 3 h. The reactions were monitored using GC-MS.

Transesterification of Alcohols. In a Schlenk tube, 5 mmol of alcohol, 6 mmol of ester, and 30 mg of nanocatalyst (KCC-1-N500) were mixed in toluene (10 mL) under argon. This reaction mixture was then heated at 110 °C in an oil bath for 3 h.

RESULTS AND DISCUSSION

Synthesis and Characterization of Nitridated KCC-1.

The first step in the preparation of these solid bases was postsynthetic nitridation of KCC-1 by ammonolysis under a flow of ammonia (NH_3) gas (Scheme 1). To optimize the nitridation temperature, a wide range of nitridated KCC-1 materials was prepared by conducting ammonolysis at different temperatures (nitridated samples were named KCC-1-N, followed by the nitridation temperature). Temperature plays a significant role in the magnitude of nitridation and thus in the nitrogen content and textural properties of these materials (Table 1). The nitrogen content in these materials increased with the nitridation temperature.

Table 1. Textural Properties of Nitridated KCC-1

sample name	BET surface area (m^2/g)	Langmuir surface area (m^2/g)	BJH pore volume (cm^3/g)	nitrogen content (wt %)
KCC-1	669	964	1.27	0
KCC-1-N400	650	980	1.04	1.13
KCC-1-N500	646	985	1.08	1.60
KCC-1-N600	639	978	1.28	1.83
KCC-1-N700	633	968	1.02	3.23
KCC-1-N800	578	883	0.91	5.63
KCC-1-N900	565	861	1.15	7.29
KCC-1-N1000	497	757	1.05	14.03
KCC-1-N1100	426	649	0.90	20.68

A typical type IV isotherm with hysteresis was observed for nitridated KCC-1 at different temperatures (Figure 1). Unlike SBA-15 or MCM-41, the surface area of KCC-1 did not decrease drastically due to its robust nature. However, a slight reduction in surface area was observed until 700 °C, with more pronounced reductions from 800 to 1100 °C (Table 1). Furthermore, little change was observed in the pore volumes of

nitridated KCC-1. These results indicate that the ammonolysis of KCC-1 resulting from thermal treatment with ammonia does not occur at the expense of its textural properties.

The morphology of these nitridated materials was then studied by transmission electron microscopy (TEM) (Figure 2) and scanning electron microscopy (SEM) (Figure 3). Figure 2 shows that all nitridated derivatives of KCC-1 consists of spheres with diameters ranging from 300 to 600 nm with a fibrous morphology. However, SEM images in Figure 3 shows that fibers of KCC-1 and its nitridated version are more like the petal of a flower than a hairy fiber. This morphology is well preserved even after nitridation with no detectable changes in their fibrous morphology. However, a few broken spheres were observed at higher nitridation temperatures (Figure 3f–h).

An X-ray photoelectron spectroscopy (XPS) study showed peaks at binding energies of about -103 , -154 , -285 , -400 , and -533 eV for Si 2p, Si 2s, C 1s, N 1s, and O 1s ionization, respectively (Figure 4a). The XPS results revealed changes in these binding energies with increases in the nitridation temperature. With the increase in nitridation temperature, the binding energy for N 1s decreases as amine protons are replaced with silicon atoms, which are more electropositive (Figure 4b). Similarly, the binding energy of the Si 2p electrons also decreases as electronegative oxygen atoms are replaced with comparatively less electronegative nitrogen atoms (Figure 4c). No significant changes were observed in the binding energies of O 1s electrons (Figure 4d). Since XPS is a surface sensitive technique, the nitrogen contents measured by XPS are generally not consistent with the results from CHN analyses. However, in this case, due to the fibrous nature of KCC-1, X-rays penetrated the nanospheres, and the N-content values from XPS closely matched the results obtained using the CHN technique.

Amine functionalization of KCC-1 was also examined using ^1H -MAS NMR and FT-IR spectroscopy techniques. From the ^1H -MAS NMR spectra of various KCC-1-N materials (Figure 5a), it can be clearly seen that the signal intensity for silanol protons at 1.7 ppm decrease, while the signal intensity at 0.6 ppm for amines increase, indicating continuous conversion of silanols to amines with increasing nitridation temperature.

The behavior described above was also examined using ^{29}Si -MAS NMR spectroscopic analysis of the KCC-1-N series (Figure 5b). The spectrum of pure KCC-1 displays three peaks at -94 , -104 , and -113 ppm, which can be attributed to Q^2 ($\text{SiO}_2(\text{OH})_2$), Q^3 (SiO_3OH), and Q^4 (SiO_4) sites, respectively. When KCC-1 was nitridated at various temperatures, the peaks for Q^2 and Q^3 started to disappear, and the nitridated materials developed an additional peak at approximately -90 ppm, which can be attributed to a surface amino group $\text{SiO}_3(\text{NH}_2)$. The intensity of this peak increased up to 700 °C. However, when

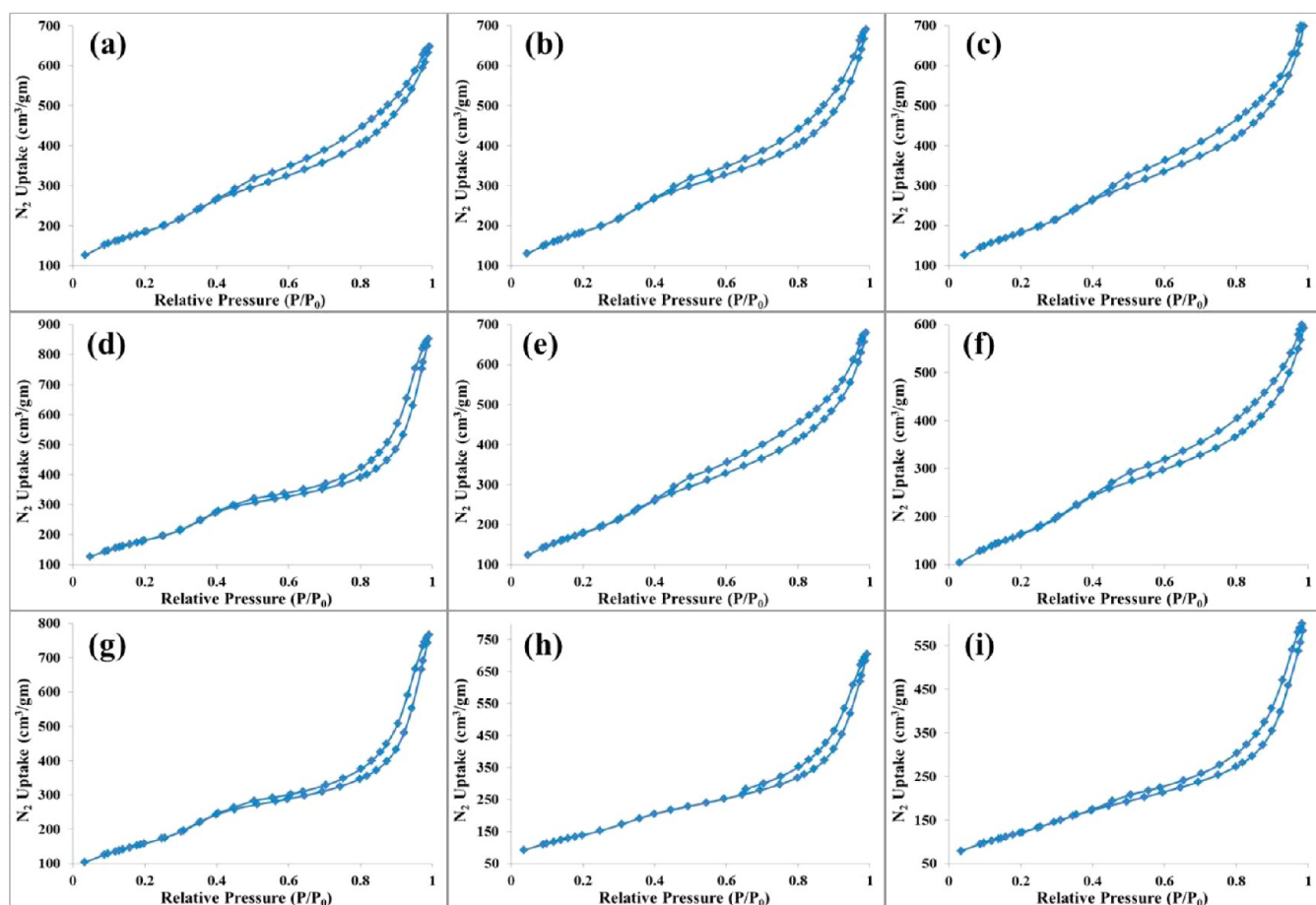


Figure 1. Nitrogen adsorption/desorption isotherms on (a) KCC-1, (b) KCC-1-N400, (c) KCC-1-N500, (d) KCC-1-N600, (e) KCC-1-N700, (f) KCC-1-N800, (g) KCC-1-N900, (h) KCC-1-N1000, and (i) KCC-1-N1100.

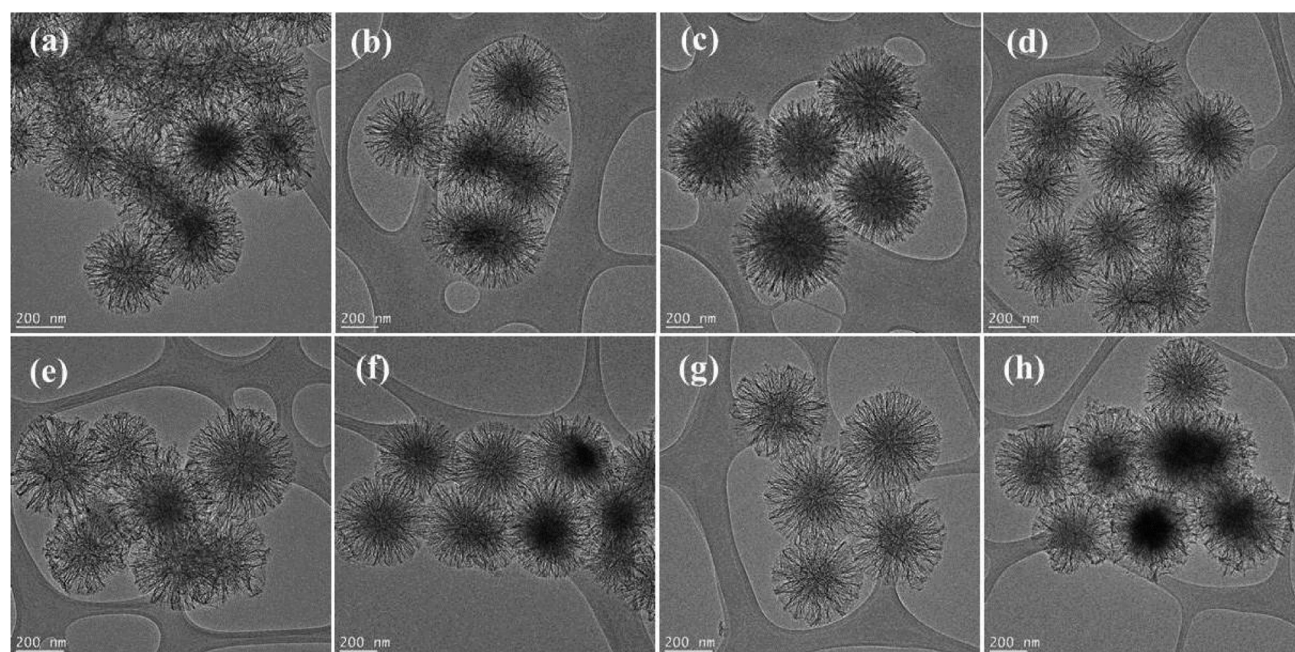


Figure 2. HR-TEM images of (a) KCC-1-N400, (b) KCC-1-N500, (c) KCC-1-N600, (d) KCC-1-N700, (e) KCC-1-N800, (f) KCC-1-N900, (g) KCC-1-N1000, and (h) KCC-1-N1100.

the nitridation temperature was further increased up to 1100 °C, a reduction in the intensity of this peak was observed, and

some broad peaks appeared at approximately -70 ppm, most likely for silazane ($-\text{Si}-\text{NH}-\text{Si}-$) species. This result

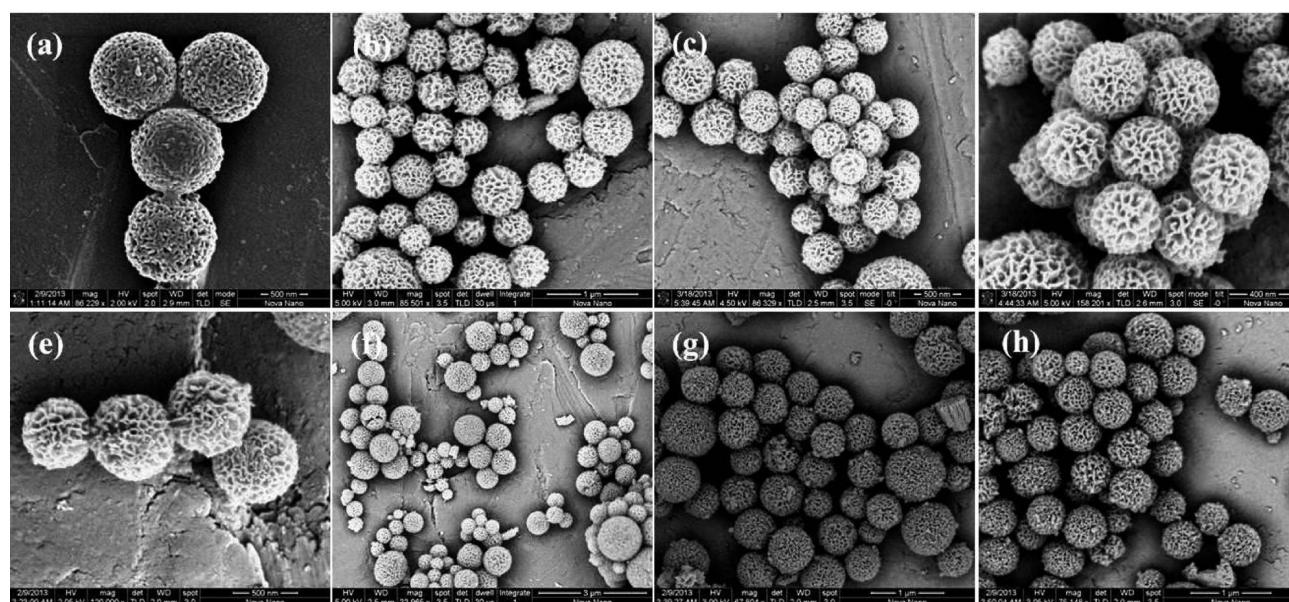


Figure 3. SEM images of (a) KCC-1-N400, (b) KCC-1-N500, (c) KCC-1-N600, (d) KCC-1-N700, (e) KCC-1-N800, (f) KCC-1-N900, (g) KCC-1-N1000, and h) KCC-1-N1100.

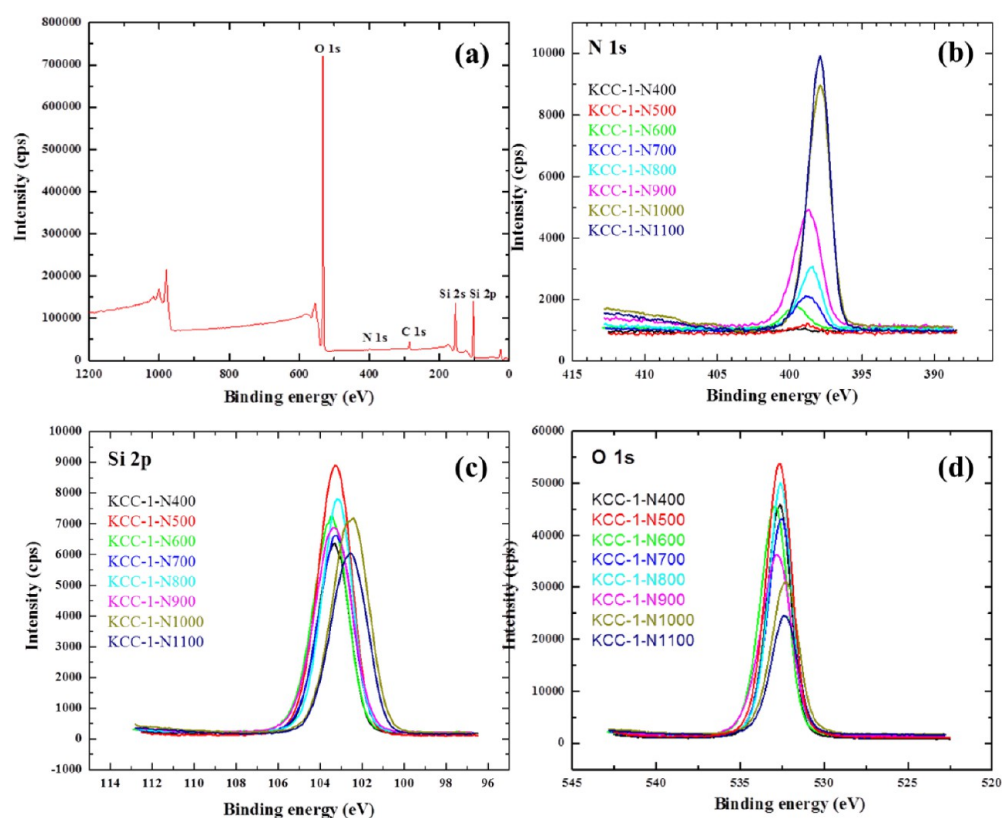


Figure 4. XPS spectra of (a) KCC-1-N500, (b) N 1s, (c) Si 2p, and (d) O 1s of nitridated KCC-1 series.

indicates that above 700 °C, surface amines merged into the bulk silica matrix and generated various thermally stable silazane species.

Similarly, from the FT-IR spectra of various KCC-1-N materials (Figure 6), an increase in nitridation temperature caused the intensity of the IR band for silanols at 3741 cm^{-1} to decrease, and new bands appeared corresponding to NH_2 stretching at 3516 and 3444 cm^{-1} and NH_2 bending at 1552 cm^{-1} . The intensity of these bands (with respect to the silanol

band) increased with nitridation temperature, indicating progressive ammonolysis of silanol to amines. Low-angle X-ray diffraction (XRD) patterns shows broad diffraction lines, indicating ordered mesostructure with very low ordering of nitridated silica (Figure S1, Supporting Information).

Knoevenagel Condensation Reactions. The basicity of the as-synthesized nitridated KCC-1 was probed using a well-known probe reaction: Knoevenagel condensation reactions (Scheme 2) of benzaldehyde with ethyl cyanoacetate (probe

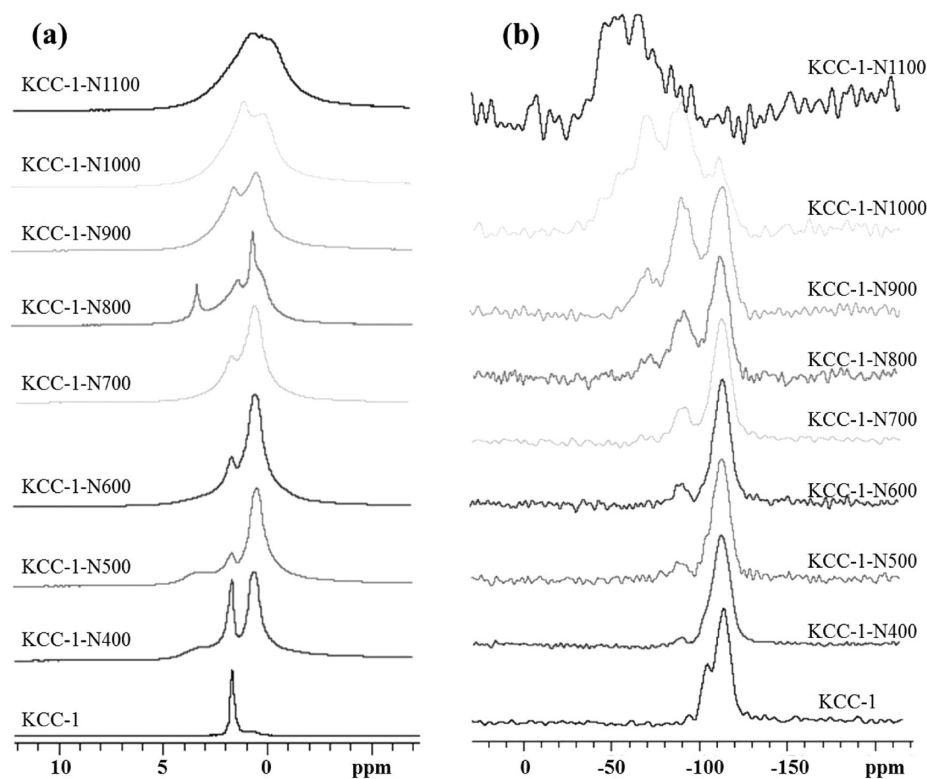


Figure 5. (a) ^1H and (b) ^{29}Si MAS NMR spectra of the KCC-1-N series. (The additional signal around 4 ppm in the case of ^1H KCC-1-N800 is due to exposure to moisture.)

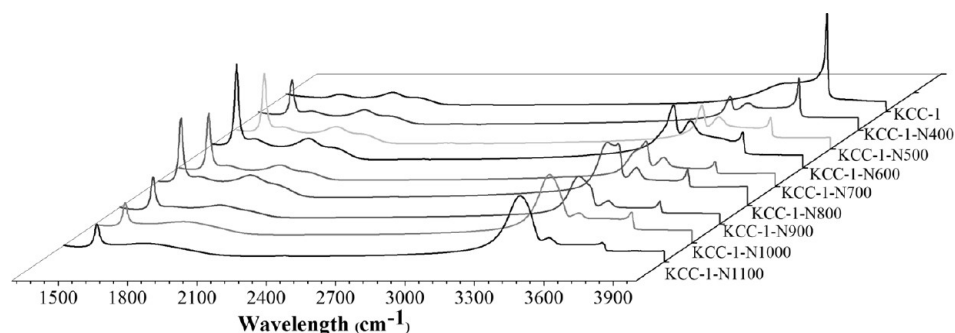
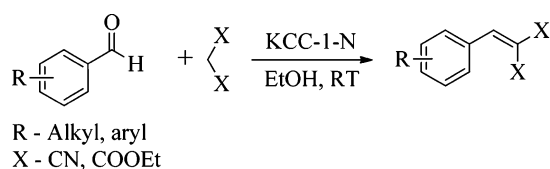


Figure 6. FT-IR spectra of the KCC-1-N series.

Scheme 2. Knoevenagel Condensation of Aldehydes



molecules). Five mmol of benzaldehyde, 6 mmol of ethyl cyanoacetate, and 30 mg of KCC-1-N series material as a catalyst in 10 mL of ethanol were stirred at room temperature. Samples of the reaction mixture were then periodically withdrawn and analyzed using gas chromatography–mass spectroscopy (GC-MS) to measure conversion as a function of the reaction time.

Figure 7 shows the catalytic activities of the KCC-1-N series for the Knoevenagel condensation of benzaldehyde and ethyl cyanoacetate. First, the reaction was conducted using pure KCC-1, and a negligible (less than 4%) conversion was

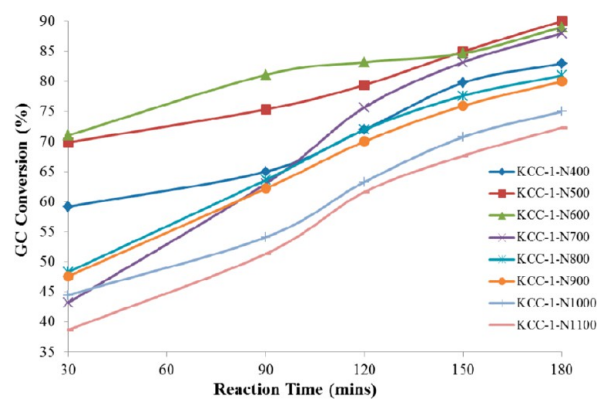


Figure 7. Knoevenagel condensation reactions of ethyl cyanoacetate with benzaldehyde catalyzed by the KCC-1-N series.

observed even after 24 h of reaction time. The absence of catalytic activity prior to nitridation indicates that the intrinsic

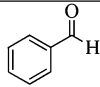
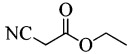
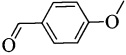
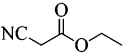
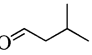
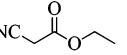
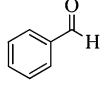
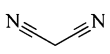
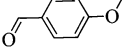
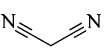
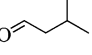
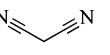
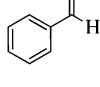
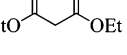
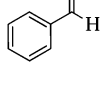
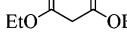
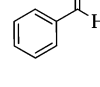
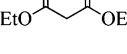
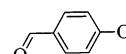
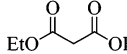
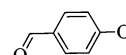
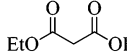
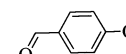
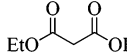
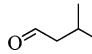
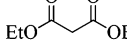
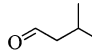
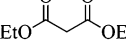
basicity associated with KCC-1 silica is not sufficient to abstract the acidic proton and initiate the catalytic cycle. However, when nitrated KCC-1 samples were used as catalysts, the Knoevenagel condensation reactions proceeded (Figure 7) with various catalytic activities, which were mainly influenced by nitridation temperatures. The KCC-1-N400 to N700 materials converted over 75% of benzaldehyde in 3 h of reaction time. Notably, KCC-1-N500 exhibited high catalytic activity, and 90% conversion was achieved with a selectivity of 100% within 3 h of reaction time. However, in the cases of KCC-1-N800 to N1100, although the nitrogen contents were higher, the conversions were lower than KCC-1-N500. These results are mainly possible because the majority of nitrogen species are predominantly located in narrow pores, which are inaccessible to reactants.³⁵

Thus, although the nitrogen content of these materials increased with nitridation temperature (Table 1), the nitrogen content was not reflected in the enhancement of activity above a nitridation temperature of 700 °C. This behavior indicates that the basicity of these materials depends not only on the nitrogen contents but also more importantly on the types of nitrogen species. It has been reported that the ammonolysis of silanol groups of silica occurs above 400 °C and proceeds via two different pathways.²⁵ The first pathway is a substitution reaction in which silanols are converted into primary amines. The second pathway, which occurs predominately at higher temperatures, involves dissociative reactions of ammonia with siloxane bridges forming silazane ($-\text{Si}-\text{NH}-\text{Si}-$) species with secondary amines. Additionally, at higher temperatures, due to their limited thermal stability, $-\text{NH}_2$ groups are incorporated inside the structure in the form of stable silazanes.¹⁶ This behavior was studied by MAS NMR (Figure 5) and XPS (Figure 4) analysis of the KCC-1-N series.

The temperature-dependent activity of these nitrated materials can be explained by two phenomena. (i) With the increase in nitridation temperature, although the nitrogen content increased (Table 1), the number of primary amines decreased, and more secondary amines, in the form of silazanes, formed (Figures 2 and 4). These silazanes are located inside the silica framework, limiting their accessibility and thus the basicity of these sites.^{16,25} KCC-1-N500 has an optimum nitrogen content as well as more active basic sites compared to its analogues that are nitrated at high temperatures. (ii) Both basic and acidic sites are required to promote Knoevenagel condensation reactions.^{36,37} Therefore, not only basic amine sites but also acidic silanol sites promote the catalytic activity of these materials. In the case of nitrated KCC-1-N materials, we observed silanol sites, which diminished with increasing nitridation temperature (Figure 6, FT-IR). This result was confirmed by ^1H MAS NMR³⁸ spectra (Figure 5a). Thus, KCC-1-N500 has the maximum number of basic amine sites and acidic silanol sites. As a result, KCC-1-N500 with the optimum nitrogen content and highest number of pair sites ($\text{Si}-\text{NH}_2$ and $\text{Si}-\text{OH}$) shows the highest catalytic activity in the KCC-1-N series.

To study the generality of the developed catalytic protocol, several other substrates were evaluated using Knoevenagel condensation reactions. In almost every case, excellent conversion was observed. A wide range of aldehydes (aliphatic, aromatic, and heterocyclic) as well as active methylene compounds reacted well with moderate to excellent conversions (Table 2). In the case of less reactive diethyl malonate, none of the aldehydes reacted under optimum conditions

Table 2. Knoevenagel Condensation of Various Substrates

Entry	Aldehyde	Active methylene compounds	% Conversion (by GC-MS)
1			89
2			45
3			98
4			99
5			77
6			99
7			0
8			25 ^b
9			52 ^c
10			0
11			34 ^b
12			47 ^c
13			0
14			94 ^b

^aReactions were carried out with 5 mmol of aldehyde, 6 mmol of active methylene substrates, and 30 mg of nanocatalyst (KCC-1-N500) at room temperature for 3 h, in ethanol (10 mL). ^bCatalyst 90 mg, temperature 80 °C, ethanol as a solvent, and reaction time 24 h. ^cCatalyst 90 mg, DMF as a solvent, temperature 80 °C, and reaction time 24 h.

(Table 2, entries 7, 10, and 13). However, by simply increasing the catalyst amount (90 mg), reaction temperature (80 °C), and reaction time (24 h), the aldehydes underwent moderate conversion (Table 2, entries 8, 11, and 14), which was further

increased by changing the solvent to dimethylformamide (DMF) (Table 2, entries 9 and 12).

To compare the activity of this optimized base (KCC-1-N500) with known solid bases (using SBA-15 and MCM-41 silica as a support), the Knoevenagel condensation reaction of benzaldehyde with a difficult substrate, diethyl malonate (Scheme 2, $X = \text{COOEt}$), was studied (Table 3). This reaction

Table 3. Comparison between Nitridated KCC-1 and Conventional Nitridated Bases

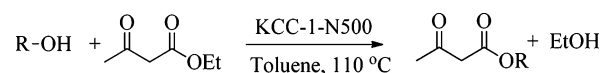
sample	KCC-1-N500	NSBA ²⁹	Me-NSBA ²⁹	Me-NMCM ²⁹
N content wt % (mmol/g)	1.6 (1.14)	24.2 (17.3)	18.4 (13.1)	1.1 (0.76)
catalysts amount mg (N mmol)	90 (0.10)	20 (0.34)	20 (0.26)	20 (0.015)
conversion in 24 h (%)	52	0	15	9

is more challenging due to the presence of a less acidic proton in diethyl malonate as well as its bulky nature, which requires stronger basic sites and more free volume (wider pores) around these sites to penetrate and react.¹⁵ Most nitridated bases were not able to catalyze this reaction.²⁹

Ammoniated NSBA-15 showed no catalytic activity (Table 3).²⁹ Even a material that recently was described as the best known solid base,²⁹ i.e., N-methylated SBA-15 (Me-NSBA), converted only 15% of this substrate. Me-NMCM converted even less, only 9% of the substrate. Notably, KCC-1-N500 showed superior activity compared to these materials, with 52% conversion. Importantly, this high activity was achieved by simply changing the support from conventional materials to KCC-1 without any chemical modification, making this a sustainable protocol. This enhancement in activity is explained by the better accessibility of amines in KCC-1-N500 as well as the presence of acidic silanols. Additionally, due to the flexible nature of KCC-1 fibers,^{30–34} pore diameters can expand during reactions, which enables diethyl malonate to easily penetrate and approach the basic amine sites. These results confirm the advantages of the fibrous morphology of KCC-1 over the tubular porous morphology of SBA-15 and MCM-41.

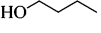
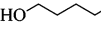
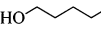
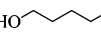
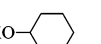
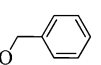
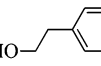
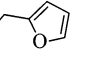
Transesterification Reactions. To study the broad applicability of this catalyst, transesterification reactions of esters with various alcohols were studied using KCC-1-N500 (Scheme 3) and compared with a well-known carbon nitride

Scheme 3. Transesterification of Ethyl Acetoacetate with Various Alcohols



catalyst.⁵ Transesterification is an important protocol for ester synthesis, which is generally catalyzed by acids and bases. Using KCC-1-N500 as a catalyst, almost every type of alcohol, including aliphatic, aromatic, and heterocyclic, was efficiently converted to a corresponding ester with good to excellent yield (Table 4). Importantly, compared to the activity of one of the well-known catalysts, carbon nitride (MCN-3),⁵ KCC-1-N500 show multifold increases in activity and turnover number (TON) (Table 4). The catalyst was also recyclable up to five times; however, conversion was decreased from 99% (Table 4,

Table 4. Transesterification of Ethyl Acetoacetate with Various Alcohols Using KCC-1-N500 and Comparison with MCN-3

Entry	Alcohols	% Conversion (by GC-MS)	TON (in 3 h)	
			Catalyst KCC-1-N500	Catalyst MCN-3 ⁵
1		76	110	1.9
2		99	144	NR
3		65	94	3.61
4		69	100	3.18
5		64	91.8	2.76
6		49	71	3.4
7		43	62	NR
8		55	80	3.29

^aReactions were carried out with 5 mmol of alcohol, 6 mmol of ester, and 30 mg of nanocatalyst (KCC-1-N500) at 110 °C for 3 h in toluene (10 mL). NR: not reported.

entry 2) to 45% (2nd cycle) and gradually to 30% in the fifth cycle. Catalyst fibrous morphology and other textural properties remained unchanged (Figure S2, Supporting Information).

CONCLUSIONS

In conclusion, we have developed a novel base by nitridation of KCC-1 and showed the advantages of its fibrous morphology and highly accessible surface area. Nitridated KCC-1 was found to be a very active and robust base for Knoevenagel condensation reactions of various aldehydes, even with challenging substrates. The as-synthesized catalysts were also found active for the transesterification of esters with a wide range of alcohols and showed multifold enhancement in activity than the known catalysts. This enhancement in activity was explained by the presence of both basic (amines) and acidic (silanols) sites as well as excellent accessibility of these sites due to the open and flexible fibrous structure of KCC-1 (unlike MCM-41 or SBA-15), which helped substrates to easily penetrate and interact with basic amine sites and in turn accelerated the overall reactions.

ASSOCIATED CONTENT

Supporting Information

Low-angle XRD of nitridated materials and SEM and TEM of used recycled catalyst. This material is available free of charge via the Internet at <http://pubs.acs.org>.

AUTHOR INFORMATION

Corresponding Author

*E-mail: vivekpol@tifr.res.in.

Notes

The authors declare no competing financial interest.

■ REFERENCES

- (1) Yokoi, T.; Kubota, Y.; Tatsumi, T. Amino-functionalized mesoporous silica as base catalyst and adsorbent. *Appl. Catal., A* **2012**, *421*–422, 14–37.
- (2) Ono, Y. Solid base catalysts for the synthesis of fine chemicals. *J. Catal.* **2003**, *216*, 406–415.
- (3) Hattori, H. Basic catalysts and fine chemicals. *Stud. Surf. Sci. Catal.* **1993**, *78*, 35–49.
- (4) Sharma, K.; Asefa, T. Efficient bifunctional nanocatalysts by simple postgrafting of spatially isolated catalytic groups on mesoporous materials. *Angew. Chem., Int. Ed.* **2007**, *46*, 2879–2882.
- (5) Jin, X.; Balasubramanian, V. V.; Selvan, S. T.; Sawant, D. P.; Chari, M. A.; Lu, G. Q.; Vinu, A. Highly ordered mesoporous carbon nitride nanoparticles with high nitrogen content: A metal-free basic catalyst. *Angew. Chem., Int. Ed.* **2009**, *48*, 7884–7887.
- (6) Shiju, N. R.; Alberts, A. H.; Khalid, S.; Brown, D. R.; Rothenberg, G. Mesoporous silica with site-isolated amine and phosphotungstic acid groups: A solid catalyst with tunable antagonistic functions for one-pot tandem reactions. *Angew. Chem., Int. Ed.* **2011**, *50*, 9615–9619.
- (7) Li, T.-T.; Sun, L.-B.; Liu, X.-Y.; Sun, Y.-H.; Song, X.-L.; Liu, X.-Q. Isolated lithium sites supported on mesoporous silica: A novel solid strong base with high catalytic activity. *Chem. Commun.* **2012**, *48*, 6423–6425.
- (8) Lednor, P. W. Synthesis, stability, and catalytic properties of high surface area silicon oxynitride and silicon carbide. *Catal. Today* **1992**, *15*, 243–261.
- (9) Lednor, P. W.; de Ruiter, R. The use of a high surface area silicon oxynitride as a solid, basic catalyst. *Chem. Commun.* **1991**, 1625–1626.
- (10) Chorley, R. W.; Lednor, P. W. Synthetic routes to high surface area non-oxide materials. *Adv. Mater.* **1991**, *3*, 474–485.
- (11) Grange, P.; Bastians, P.; Conanec, R.; Marchand, R.; Laurent, Y. Influence of nitrogen content of a new aluminophosphate oxynitride catalyst: AIPON in Knoevenagel condensation. *Appl. Catal., A* **1994**, *114*, 191–196.
- (12) Fripiat, N.; Parvulescu, V.; Parvulescu, V. I.; Grange, P. Role of nitrogen on the acid–base properties of zirconophosphate (ZrPON) oxynitride catalysts. *Appl. Catal., A* **1999**, *181*, 331–346.
- (13) Climent, M. J.; Corma, A.; Fornes, V.; Frau, A.; Guil-Lopez, R.; Iborra, S.; Primo, J. Acidity studies of fluid catalytic cracking catalysts by microcalorimetry and infrared spectroscopy. *J. Catal.* **1996**, *163*, 392–398.
- (14) Haskouri, J. E.; Cabrera, S.; Sapina, F.; Latorre, J.; Guillem, C.; Beltran-Porter, A.; Beltran-Porter, D.; Marcos, M. D.; Amoros, P. Ordered mesoporous silicon oxynitrides. *Adv. Mater.* **2001**, *13*, 192–195.
- (15) Hasegawa, T.; Krishnan, C. K.; Ogura, M. Promising catalytic performance and shape-selectivity of nitrogen-doped siliceous MFI zeolite for base-catalyzed reactions. *Microporous Mesoporous Mater.* **2010**, *132*, 290–295.
- (16) Hayashi, F.; Ishizu, K.; Masakazu, I. Effect of pore structure on the nitridation of mesoporous silica with ammonia. *Eur. J. Inorg. Chem.* **2010**, *15*, 2235–2243.
- (17) Hayashi, F.; Ishizu, K.; Iwamoto, M. Fast and almost complete nitridation of mesoporous silica mcm-41 with ammonia in a plug-flow reactor. *J. Am. Ceram. Soc.* **2010**, *93*, 104–110.
- (18) Wang, J.; Liu, Q. Structural change and characterization in nitrogen-incorporated SBA15 oxynitride mesoporous materials via different thermal history. *Microporous Mesoporous Mater.* **2005**, *83*, 225–232.
- (19) Chino, N.; Okubo, T. Nitridation mechanism of mesoporous silica: SBA-15. *Microporous Mesoporous Mater.* **2005**, *87*, 15–22.
- (20) Xia, Y.; Mokaya, R. Ordered mesoporous MCM-41 silicon oxynitride solid base materials with high nitrogen content: synthesis, characterisation and catalytic evaluation. *J. Mater. Chem.* **2004**, *14*, 2507–2515.
- (21) Wan, K.; Liu, Q.; Zhang, C.; Wang, J. The basicity and catalytic activity of ordered mesoporous silicon nitride oxide. *Bull. Chem. Soc. Jpn.* **2004**, *77*, 1409–1414.
- (22) Xia, Y.; Mokaya, R. Highly ordered mesoporous silicon oxynitride materials as base catalysts. *Angew. Chem., Int. Ed.* **2003**, *42*, 2639–2644.
- (23) Asefa, T.; Kruk, M.; Coombs, N.; Grondy, H.; MacLachlan, M. J.; Jaroniec, M.; Ozin, G. A. Novel route to periodic mesoporous aminosilicas, pmas: Ammonolysis of periodic mesoporous organo-silicas. *J. Am. Chem. Soc.* **2003**, *125*, 11662–11673.
- (24) Kaskel, S.; Schlichte, K.; Zibrowius, B. Pore size engineering of mesoporous silicon nitride materials. *Phys. Chem. Chem. Phys.* **2002**, *4*, 1675–1681.
- (25) Fink, P.; Muller, B.; Rudakoff, G. Ammoniation and nitridation of highly disperse silica. *J. Non-Cryst. Solids* **1992**, *145*, 99–104.
- (26) Habraken, F. H. P. M.; Kuiper, A. E. T.; Tamminga, Y.; Theeten, J. B. Thermal nitridation of silicon dioxide films. *J. Appl. Phys.* **1982**, *53*, 6996–7002.
- (27) Busca, G. Bases and basic materials in chemical and environmental processes. Liquid versus solid basicity. *Chem. Rev.* **2010**, *110*, 2217–2249.
- (28) Ono, Y.; Baba, T. Strong solid bases for organic reactions. *Catalysis* **2000**, *15*, 1–39.
- (29) Sugino, K.; Oya, N.; Yoshie, N.; Ogura, M. A simple modification creates a great difference: New solid-base catalyst using methylated N-substituted SBA-15. *J. Am. Chem. Soc.* **2011**, *133*, 20030–20032.
- (30) Polshettiwar, V.; Cha, D.; Zhang, X.; Basset, J. M. High-surface-area silica nanospheres (KCC-1) with a fibrous morphology. *Angew. Chem., Int. Ed.* **2010**, *49*, 9652–9656.
- (31) Polshettiwar, V.; Thivolle-Cazat, J.; Taoufik, M.; Stoffelbach, F.; Norsic, S.; Basset, J. M. Hydro-metathesis of olefins: A catalytic reaction using a bifunctional single-site tantalum hydride catalyst supported on fibrous silica (KCC-1) nanospheres. *Angew. Chem., Int. Ed.* **2011**, *50*, 2747–2751.
- (32) Fihri, A.; Bouhrara, M.; Cha, D.; Almana, N.; Polshettiwar, V. Fibrous nano-silica (KCC-1)-supported palladium catalyst: Suzuki coupling reactions under sustainable conditions. *ChemSusChem* **2012**, *5*, 85–89.
- (33) Patil, U.; Fihri, A.; Emwas, A. H.; Polshettiwar, V. Silicon oxynitrides of KCC-1, SBA-15 and MCM-41: Unprecedented materials for CO₂ capture with excellent stability and regenerability. *Chem. Sci.* **2012**, *3*, 2224–229.
- (34) Fihri, A.; Bouhrara, M.; Patil, U.; Cha, D.; Saih, Y.; Polshettiwar, V. Fibrous nano-silica supported ruthenium (KCC-1/Ru): A sustainable catalyst for the hydrogenolysis of alkanes with good catalytic activity and lifetime. *ACS Catalysis* **2012**, *2*, 1425–1431.
- (35) Wu, G.; Jiang, S.; Li, L.; Zhang, F.; Yang, Y.; Guan, N.; Mihaylov, M.; Knözinger, H. Physico-chemical characterization of nitrated mesoporous silicon MCM-41. *Microporous Mesoporous Mater.* **2010**, *135*, 2–8.
- (36) Inaki, Y.; Kajita, Y.; Yoshida, H.; Ito, K.; Hattori, T. New basic mesoporous silica catalyst obtained by ammonia grafting. *Chem. Commun.* **2001**, 2358–2359.
- (37) Narasimharao, K.; Hartmann, M.; Thiel, H. H.; Ernst, S. Novel solid basic catalysts by nitridation of zeolite beta at low temperature. *Microporous Mesoporous Mater.* **2006**, *90*, 377–383.
- (38) Bendjeriou-Sedjerari, A.; Pelletier, J. D.; Abou-Hamad, A. E.; Emsley, L.; Basset, J. M. A well-defined mesoporous amine silica surface via a selective treatment of SBA-15 with ammonia. *Chem. Commun.* **2012**, *48*, 3067–3069.